Impact of Component Size on Plug-In Hybrid Vehicle Energy Consumption Using Global Optimization

DOMINIK KARBOWSKI
Argonne National Laboratory
9700 South Cass Avenue, Argonne, IL 60439-4815, USA
dkarbowski@anl.gov / Tel. 1-630-252-5362 / Fax: 1-630-252-3443

CHRIS HALIBURTON, AYMERIC ROUSSEAU
Argonne National Laboratory

Abstract

Plug-in hybrid electric vehicles are a promising alternative to gas-only vehicles and offer the potential to greatly reduce fuel use in transportation. Their potential energy consumption is highly linked to the size of components. This study focuses on the impact of the electric system energy and power on control and energy consumption. Based on a parallel pre-transmission architecture, several vehicles were modeled, with an all-electric range from 5 to 40 miles on the UDDS, to illustrate various levels of available electric energy. Five others vehicles were created, with various levels of power and same battery energy. The vehicles were then simulated under optimal control on multiple combinations of cycle and distance by using a global optimization algorithm. The global optimization algorithm, based on the Bellman principle, ensures a fair comparison between different vehicles by making each vehicle operate at its maximal potential. The results from each optimization are thoroughly analyzed to highlight control patterns. The potential minimal fuel consumption that can be achieved by each of them is presented. The results can also be used to find the potential minimal greenhouse gases emissions.

Keywords: Plug-in Hybrid Electric Vehicle, Global Optimization, Battery Size, All-Electric-Range, Control Strategy

1 Introduction

Plug-in Hybrid Electric Vehicles (PHEVs) are a promising alternative to conventional gas-powered vehicles. They can, indeed, be driven in an all-electric mode (EV mode) for a relatively short distance, although long enough for most daily trips. Thanks to an internal combustion engine (ICE), a PHEV can still take advantage of the high energy density of gasoline and provide the customer with an acceptable driving range.

The electric power system, composed of the battery and the electric machine, is critical in a PHEV. Its mass has to be low enough not to significantly increase the energy consumption at the wheels. To be marketable, the cost of the electric power system has to remain within limits defined by the market. Energy and power are the two main physical characteristics impacting cost and weight. It is therefore of paramount importance to adequately size the battery and the electric machine.

This study focuses on the impact of electric power system energy and power on overall energy consumption, by comparing parallel pre-transmission PHEVs whose electric systems have various power and energy sizing. When comparing different vehicles, a bias may, however, be introduced if the control is optimized for some vehicles but not for others. Running a global optimization algorithm on the torque split between the engine and the electric machine, as well as the gear, ensures that each sizing is used at

its maximal potential. As the control is an output and no longer an input of the simulations, this allows a fair comparison.

2 PHEV Modeling and Optimization

2.1 Vehicle Data

The configuration selected for this study is a parallel pre-transmission, as shown in Figure 1. It is very similar to the one used in the DaimlerChrysler Sprinter van [1]. Only one electric machine is used for both propelling and regenerative braking. This configuration is also used in the Argonne's Mobile Advanced Automotive Testbed (MATT). MATT [2] is a rolling chassis used to evaluate component technology in a vehicle system context, and it can be used for the practical applications of this study.

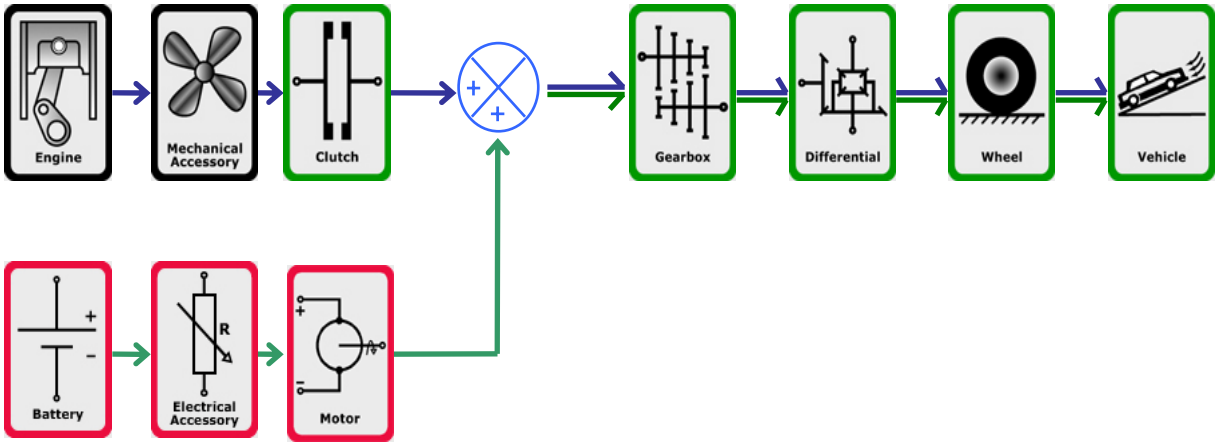

Figure 1: Component configuration of the parallel pre-transmission PHEV

The base vehicle size corresponds to a small SUV similar to a Chevrolet Equinox or a Toyota Rav4. The electric machine and battery size are variable. The main characteristics of the components are summarized in Table 1.

Table 1: Specifications of components

Component	Specifications
Engine	2.3 L, 100 kW Ford Duratec
Electric machine	Various power Based on Toyota Prius MY04 motor
Battery	Various capacity and power Based on Li-ion – Saft VL41M
Transmission	5-speed automatic transmission
	Ratio: [3.22, 2.41, 1.55, 1, 0.75]
Frontal area	2.76 m^2
Final drive ratio	3.58
Drag coefficient	0.395
Rolling resist.	0.008 (plus speed related term)
Wheel radius	0.33 m
Vehicle mass	1710 kg + motor mass + battery mass
Electric accessories	240 W

2.2 Global Optimization

2.2.1 Optimization problem

The optimization problem is defined as follows.

- *System*: parallel pre-transmission powertrain, using backward-looking model; gearbox, engine, and electric machine model use speed-torque-based efficiency look-up tables and speed-based maximal torque tables; battery model uses SOC-based open-circuit voltage and internal resistance look-up tables.
- *State*: battery state of charge (SOC), varying between 0.25 and 0.90.
- *Command*: electric machine and engine torque, gear.
- *Constraints*: following a given speed profile without exceeding each component limitations.
- *Initial condition*: a fixed value between SOC = 0.30 and SOC = 0.90.
- *Final condition*: SOC = 0.30.
- *Parameter to minimize*: fuel use.

2.2.2 Principle

The global optimization algorithm used in this study is an application of the Bellman optimality principle. It states that a sequence of decisions is optimal if, for any state and time, the following decisions are an optimal sequence of decisions for the corresponding problem having these states and times as initial conditions.

Using this algorithm requires that the time, command (engine torque), and states (SOC) be sampled to have a completely discrete system. Starting from the end (t=t_{end}-1), at each time step, the algorithm goes through all possible combinations of commands and states and, for each of them, computes the fuel use and the next state, at time t+1, by minimizing a weight function, which is, in this case, total fuel use. Assuming that the optimal path from any state at time t+1 to the end is already known, the best path from each state at time t can be computed. Global optimization has already been used in [3] and [4].

2.2.3 Interpretation of algorithm output

Energy performance for a PHEV can be defined in several ways: it can be fuel displacement, energy consumption, and GHG emissions, among others. Most of these indicators can be translated into a linear combination of thermal and electric energy use:

$$f_{a,b}\left(E_{th}, E_{el}\right) = aE_{th} + bE_{el} \text{ where } a \geq 0,\ b \geq 0$$

For instance, $f_{1,0}$ is thermal energy use, which is proportional to fuel consumption.

The optimum is achieved by minimizing $f_{a,b}\left(E_{th}, E_{el}\right)$ for any possible set of commands X. One way is to look at all the commands that, for any possible E_{el}, result in the same electric energy use E_{el}. For one of such subset of the commands space, electric energy use is constant (E_{el} = E), and $g_{th}\left(E\right)$ is the minimal thermal energy use that can be achieved within that subset:

$$g_{th} : 0 \leq E \leq E_{el}^{\max} \mapsto \min_{X, E_{el}(X)=E}\left(E_{th}\left(X\right)\right)$$

The minimum $f_{a,b}(E_{th}, E_{el})$ over all possible commands is finally solved by looking at a one-dimensional minimum problem, where the parameter is only the electric energy use:

$$\min_X\left(f_{a,b}\left[E_{th}(X), E_{el}(X)\right]\right) = \min_{0\le E\le E_{el}^{\max}}\left(a\cdot g_{th}(E) + b\cdot E\right)$$

In one given result of the global optimization, the electric energy use E_{el} is constant, while E_{th} is the minimal thermal energy use for that particular electric energy use. E_{el} is, indeed, defined by the difference between initial and final SOC. An optimization with a different initial SOC can be easily obtained without additional computation, allowing one to go through all possible ΔSOC (difference between initial and final SOC) and, therefore, all possible E_{el}. By combining results with varying electric energy use, the overall minimum can be found by using the process described above. This formalism is used to compute the minimal fuel consumption, as well as the minimal greenhouse gases emissions.

2.2.4 Limitations

The global optimization algorithm has limitations specific to the powertrain modeling that is used and to the method itself. It is important to keep them in mind when analyzing results and drawing conclusions. Global optimization sheds new light on vehicle control and is complementary to a forward-looking simulation model, such as Argonne's PSAT [5].

Because transients are not modeled, and because command and state are sampled, time-series parameters (e.g., electric machine torque) are somehow idealized.

The model does not include any control strategy: the strategy, namely the torque split between the engine and the electric machine (as well as the shifting schedule), is one of the optimization outputs. The main consequence is that the knowledge of the speed trace (and grade) is necessary to obtain the best fuel economy, and the strategy may be different from one cycle to another or even one distance to another. A possible way to apply the results into a real-world vehicle controller would be to compute the speed trace and grade before the trip starts, by using a navigation system and traffic information. Such an approach has already been experimented in the GERICO project [6] and by Nissan [7].

The algorithm only outputs the strategy that results in the optimum. The controls that lead to a result in the neighborhood of the optimum cannot be retrieved. Strategies that could have been better in some other aspects (such as their repeatability in real controllers) and that would have given very good results, although not the best, are lost in the process.

Global optimization indicates what a given powertrain can *potentially* do in terms of energy efficiency. In other words, the figures output from the optimization are obtained by using a perfect controller. They are therefore valuable in the comparison of powertrains, because they compare the powertrains used at their maximal potential, without the bias introduced by the performance of each powertrain controller.

2.3 Cycles

Three different cycles are used: the Urban Dynamometer Driving Schedule (UDDS), the Highway Fuel Economy Driving Schedule (HWFET), and LA 92. The UDDS and the HWFET are standard U.S. EPA (Environmental Protection Agency) cycles currently used for certification in the United States. LA92, also called Unified Cycle, is also issued by U.S. EPA, but it is more aggressive, as shown in Table 2, and is supposed to be more representative of current driving habits.

Table 2: Main characteristics of the cycles used in the study

	Unit	UDDS	HWFET	LA92
Duration	s	1372	764	1435
Average speed	m/s	8.9	21.6	11.0
Average acceleration	m/s^2	0.5	0.2	0.7

The distances used in this study are 10, 20, and 40 mi (respectively, 16.1, 32.2, and 64.4 km). The HWFET and LA92 are 10 mi long each, so they were repeated once, twice, and four times to get those distances. Because the UDDS is 7.5 mi (12 km), the cycle is repeated several times and then cut to be 10, 20, and 40 mi long (the cut is done at points where vehicle speed is zero).

3 Control Analysis

The global optimization algorithm outputs the optimal solution for given initial and final state (i.e., SOC). Because of the structure of the algorithm, getting a solution for the same final SOC and a different initial SOC does not require additional computations. For one run of the algorithm, it is possible to have the optimal control and minimal fuel consumption for various variations of SOC (ΔSOC). A ΔSOC of zero means the final and initial SOC are equal to 0.3: it is a charge-sustaining (CS) mode because no electric energy from the grid is consumed. On the other hand, ΔSOC of 0.6 means the battery is fully depleted from 0.9 to 0.3 of SOC.

A given ΔSOC can be associated with a "plug-to-wheel" electric energy: the amount of electric energy the grid has to provide to enable battery SOC to return to its initial value. To compute this electric energy, the charging current is assumed to be 15 A, while the charger efficiency is 0.9. Divided by the driven distance, it gives the electric consumption, in Wh/km.

In the following subsections, the analysis of the output of global optimization for a vehicle sized in PSAT to run 20 mi in EV mode on the UDDS (called hereafter 20AER) highlights the patterns behind the optimal control.

3.1 Engine-On Events

In real-world powertrain controllers, the decision to turn the engine on is often linked to the power demand at the wheels: when the power demand is above a given threshold, the engine turns on. A good indication of that threshold is the power demand at the wheels above which the probability of the engine being on is higher than 0.95 It is hereafter called *wheel power threshold*. Figure 2 shows the wheel power threshold for various cycles (differentiated by line style) and various distances (differentiated by line colors/shade). The wheel power threshold increases linearly as a function of electric consumption: the more electric energy is used, the less the engine operates, and the "later" (in terms of power) it starts. The influence of cycle type appears to be minimal.

Longer driven distance results in lower maximal electric consumption, since the total energy available from the battery is the same while distance increases. Even though the battery is fully depleted, the engine is still needed to power the vehicle.

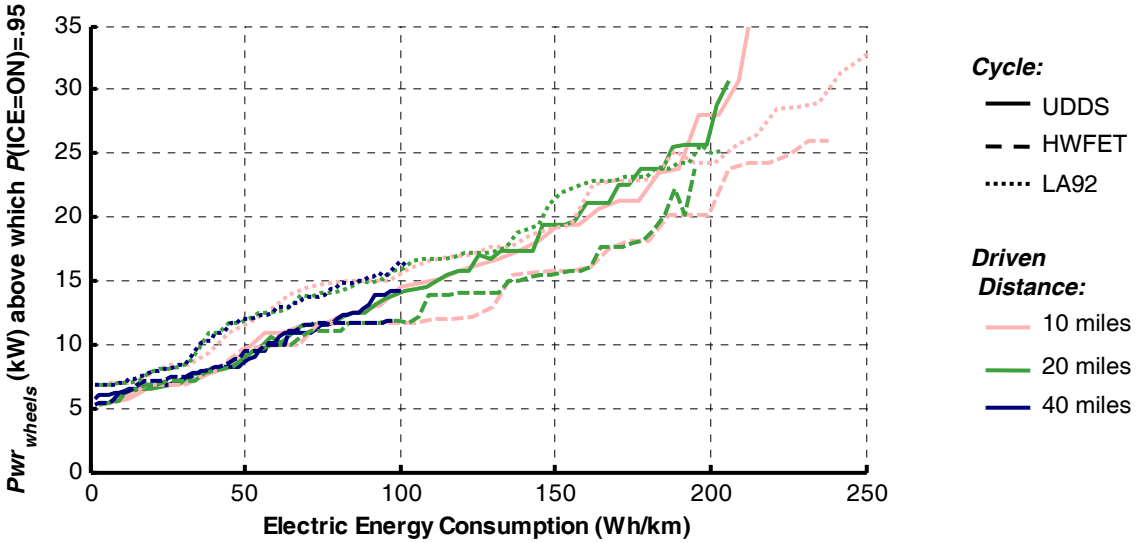

Figure 2: Power demand at the wheels above which ICE is on 95% of time – 20AER, various cycles (differentiated by colors/shade), various distances driven (differentiated by line style). *For example, lighter shade/pink dotted line corresponds to 10 mi on LA92*

3.2 Engine Operating Points

Once the engine is on, it is necessary to know how it operates. As shown in Figure 3, the average engine power increases linearly with the available battery energy. Although the engine is started less often, it is used at higher power values and, consequently, at higher efficiencies, as shown in Figure 4.

Figure 3 also shows that the average engine power also depends on the cycle. On more aggressive cycles, such as LA92, it is almost constant and higher than less-aggressive ones, which means that the engine operates at similar power levels in CS or CD mode. It is also interesting to observe that for high electric energy consumption, the difference in average power disappears: at around 175 Wh/km, the engine power does not depend any longer on the cycle.

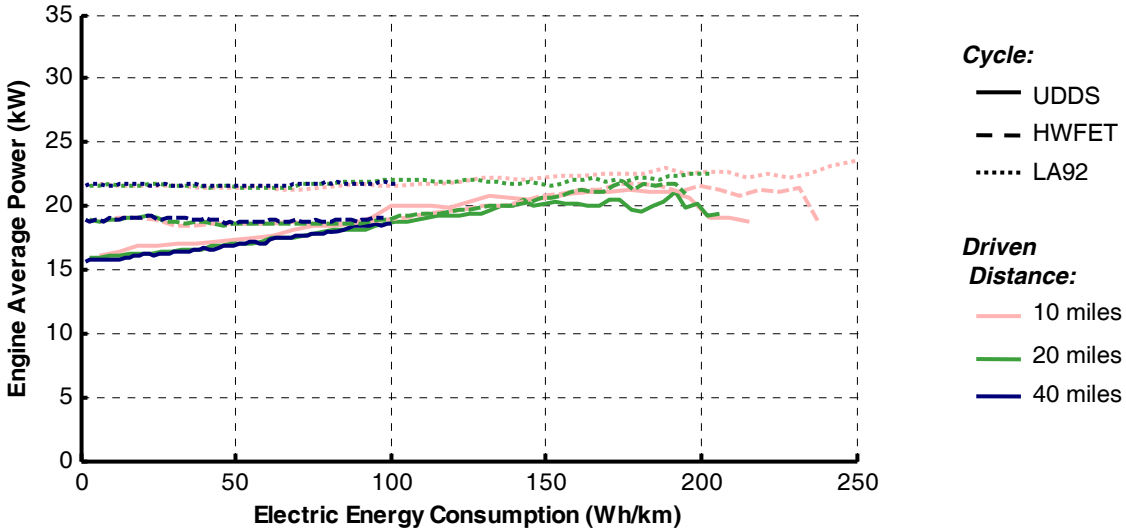

Figure 3: Engine average power – 20AER, various cycles, various distances driven

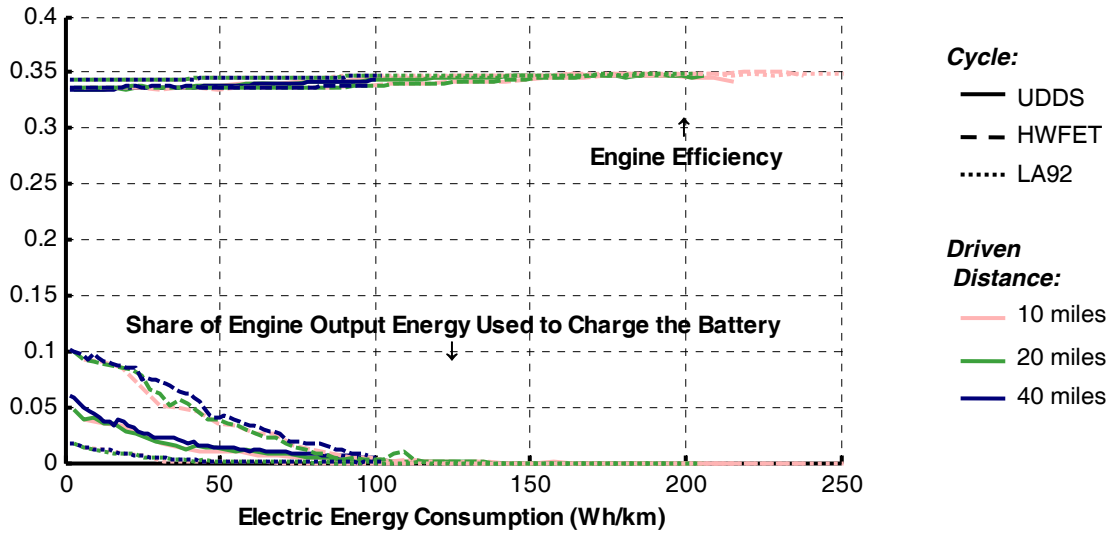

Figure 4: Engine efficiency and destination of its output – 20AER, various cycles, various distances driven

The destination of the engine output also varies in function of the cycle. On the more aggressive LA92, the engine has more opportunities to propel the vehicle while working efficiently: a lower share of its output goes to the battery, as shown in Figure 4. HWFET is the cycle with the highest share of engine output charging the battery. Because there are fewer power peaks during this cycle, the engine has to operate more often above the power required to propel the vehicle to maintain good efficiency – the extra energy is taken by the electric machine to charge the battery.

3.3 Battery SOC Management

Figure 5 compares the actual SOC depletion with a linear depletion. Linear battery depletion results in a SOC curve (as a function of time) that is a straight line. For $\Delta SOC = 0$, a linear battery depletion means a constant SOC of 0.3, whereas for $\Delta SOC = 0.6$, SOC decreases linearly from 0.9 to 0.3. A correlation of 1 means that the actual SOC curve (as a function of time) is very close to a straight line.

For low ΔSOC, or low electric consumption, the correlation is very low because there is an important SOC swing around 0.3, which is typical of a CS mode. The correlation is, however, very high for higher ΔSOC, which suggests charge-depleting mode is the optimal way to discharge the battery. The latter conclusion is valid with the driving schedules used in this study. Each of them is the result of the multiple repetition of the same cycle.

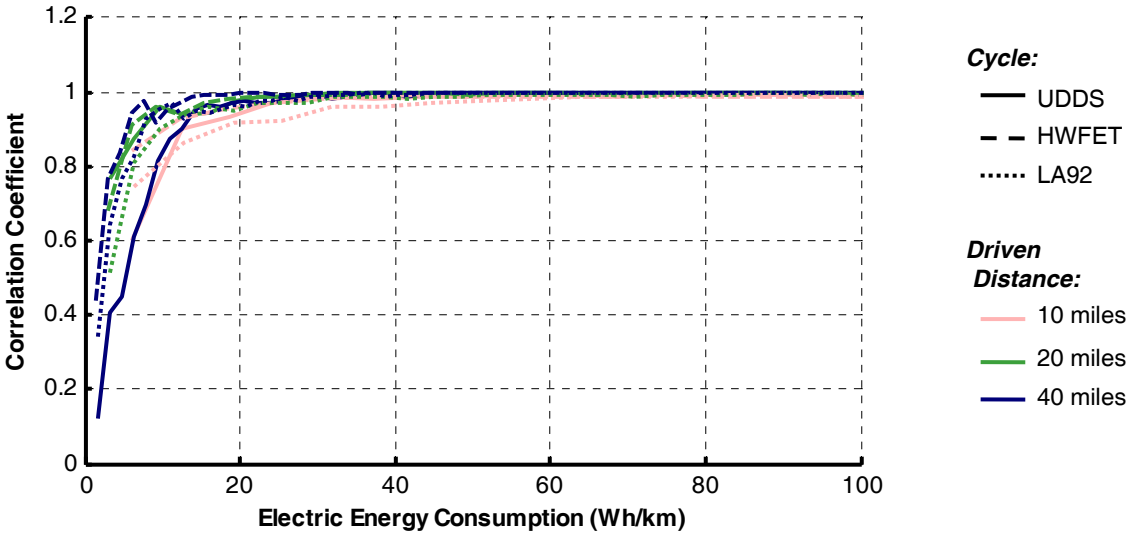

Figure 5: Correlation between SOC from actual and linear depletion – 20AER, various cycles, various distances driven

4 Influence of Energy Sizing

4.1 Vehicle Sizing

Using the vehicle described in section 2.1 as a base, an automated sizing procedure was used to generate five vehicles, with various AERs. The bus voltage has been set to approximately 200 V. To meet this requirement, 57 cells, with a nominal voltage of 3.6 V, are necessary. Battery power must be high enough to ensure the vehicle follows the UDDS speed trace, even at low SOC. Battery energy is determined by the desired AER. Power requirements affect the power per cell, while the energy requirements impact the capacity. The main parameters are summarized in Table 3.

Table 3: Main parameters of various AER vehicles

All-Electric Range (mi)	**5**	**10**	**20**	**30**	**40**
All-Electric Range (km)	8.0	16.1	32.2	48.3	64.4
Vehicle mass (kg)	1808	1823	1852	1879	1911
Battery capacity (Ah)	12	23	45	66	90
Battery usable energy (kWh)	1.5	2.9	5.5	8.1	11.1
Battery power-to-energy ratio	30.3	15.7	8.2	5.6	4.1

As battery capacity increases with AER, it is heavier. Because of the high specific energy of Li-ion technology, the variation in mass is limited – 6% between the 5-mi-AER vehicle and the 40-mi-AER vehicle. As a result, battery pack power remains relatively constant at 75 kW.

4.2 Influence on Control

The parameters used in section 3 to describe the control are not much affected by the battery energy/AER. For a given electric energy, the behavior – in its macroscopic view – of the vehicle does not depend on its AER: the engine is on above a similar wheel-power demand, while slightly higher power is output for longer-range vehicles, because of vehicle mass.

The main influence of battery energy is that for a given driven distance and vehicle, electric energy consumption is limited, as illustrated in Figure 6 (a) and (b). The same parameter is plotted (wheel power threshold), but with different abscissa. The plots in Figure 6 (a) reflect the ΔSOC, while the plots in Figure 6 (b) reflect electric energy consumption. The maximal depletion on the 10-AER vehicle is 0.6 (from 0.9 to 0.3 SOC) and results in a maximal electric energy consumption of 110 Wh/km. The 20-AER vehicle has the same depletion, but the maximal electric consumption is about 200 Wh/km, because the vehicle runs closer to an EV mode as the higher energy battery allows it. Although the 20-AER, 30-AER, and 40-AER vehicles have similar maximal electric consumption, their maximal depletion is all the lower as the AER is high: all of them run in EV-mode, but the depletion level will be lower for higher AER.

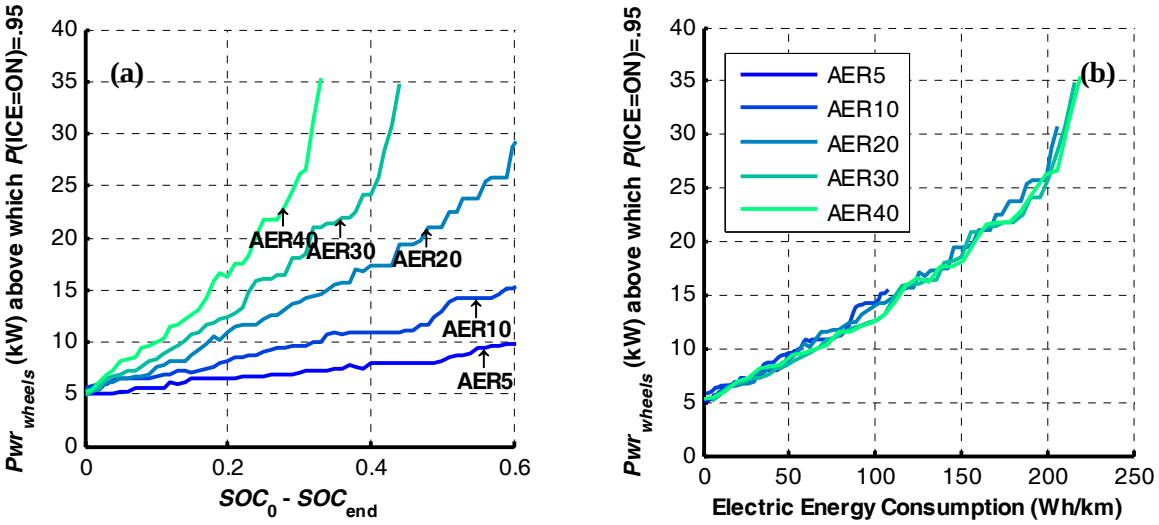

Figure 6 (a) and (b): Power demand at the wheels above which ICE is on 95% of time – various AER, UDDS, 20 mi

4.3 Influence on Fuel Economy

The influence of energy sizing on the fuel economy is similar. Even though longer-range vehicles tend to use more energy because of their weight, the difference is small enough to conclude that, for a given electric energy consumption, the influence on fuel consumption is minimal. This is shown on Figure 7.

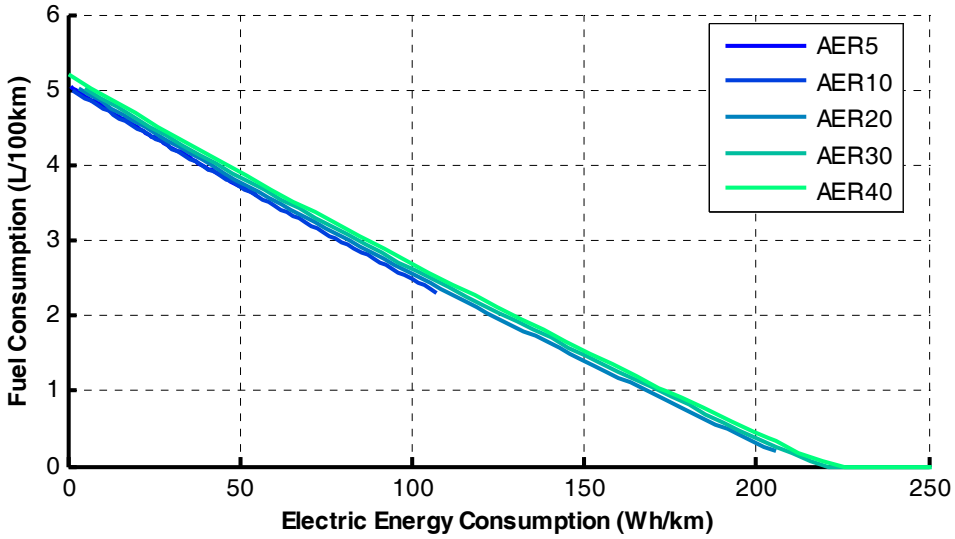

Figure 7: Fuel consumption – various AER, UDDS, 20 mi

When the focus is not on electric energy consumption, battery energy has an obvious impact. The minimal fuel consumption a vehicle can achieve on a given cycle and distance is all the lower as the battery energy is high, because it uses more electricity than fuel to propel itself, as shown in Figure 8.

Higher battery energy means higher fuel displacement (i.e., more fuel is saved in comparison to a car, the input energy for which comes from fuel only). However, when the distance driven is below the range, as for the 20-AER and 30-AER vehicles on 10 mi on UDDS, longer-range vehicles tend to be slightly penalized because of their higher mass.

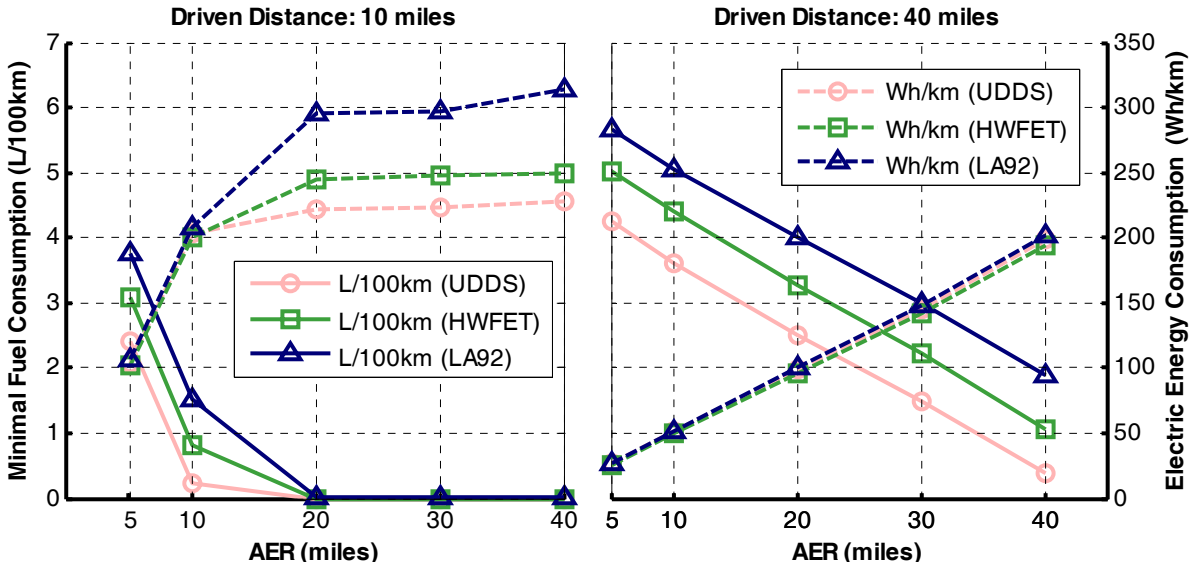

Figure 8: Minimal fuel consumption and associated electric energy consumption

4.4 Influence on Greenhouse Gas Emissions

A weight function can be applied to the global optimization algorithm results by using the formalism described in section 2.2.3. We used this feature to compute the potential well-to-wheel greenhouse gas (GHG) emissions for each vehicle.

A well-to-wheel approach not only takes into account the tailpipe emissions (pump-to-wheel) but also the emissions due to the production and the transportation of the energy source from the natural resource to the input of the vehicle (well-to-pump). GHGs include but are not limited to carbon dioxide. The assumptions related to GHG emissions data are taken from Argonne's GREET 1.8a model [8] and correspond to the 2010 American energy mix.

Electricity generation and transmission is the source of the emission of 216 g CO_2eq/MJ, whereas its use in the vehicle does not generate any. Gasoline production and distribution leads to 19.3 g CO_2eq/MJ, while its combustion in the engine generates 73.6 gCO_2eq/MJ (i.e., 92.9 gCO_2eq/MJ well-to-wheel).

Figure 9 shows GHG emissions on a 20-mi UDDS for various AER vehicles. On the basis of the data shown in Figure 9, two conclusions can be drawn. The first conclusion is that for a given electric consumption, vehicles with longer range emit slightly more GHGs because they are heavier. This is also shown on Figure 10. The second conclusion is that, for a given vehicle, the amount of electricity used may not affect emission levels much. There may be no improvement in GHG emissions between an EV mode and a CS mode.

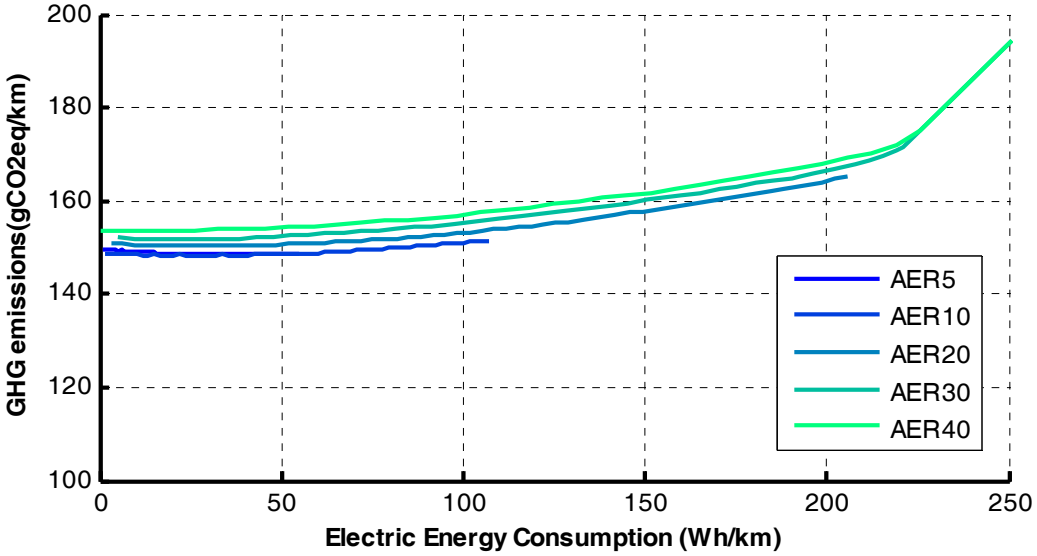

Figure 9: Greenhouse gas (GHG) emissions – various AER, UDDS, 20 mi

The electric system, from the plug to the motor output, has indeed an efficiency close to 0.7, which is almost double the engine efficiency. Those gains in efficiency are not sufficient to compensate for the high levels of GHG emissions from electricity generation and transmission in the 2010 American energy mix. The sources that will supply electricity to charge PHEVs in the future may, however, differ from the American 2010 mix. The results presented here will be updated on the basis of the outcome of ongoing studies focused on electric power generation.

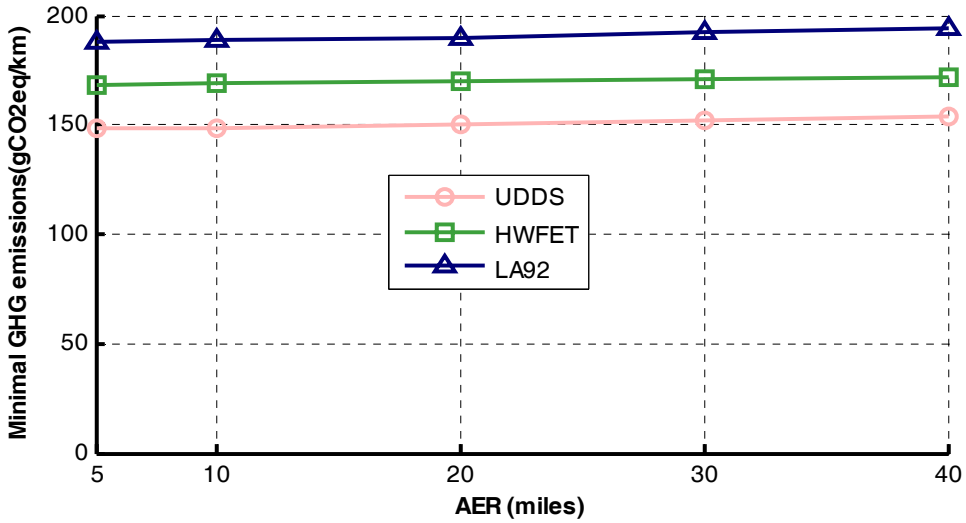

Figure 10: Minimal GHG emissions – driven distance: 20 mi

5 Influence of Power Sizing

5.1 Vehicle Sizing

To evaluate the impact of electric system power sizing on energy consumption, the 10-AER vehicle was used as a base to define vehicles with a 40% and 20% more- or less-powerful battery and electric machine while maintaining the same battery energy. The main characteristics of those vehicles are summarized in Table 4.

Table 4: Main characteristics of various power ratios for vehicles

Power Scaling Ratio	0.6	0.8	1	1.2	1.4
Vehicle mass (kg)	1785	1804	1823	1842	1860
Battery maximal power at 20%SOC	45	60	75	89	104
Battery power-to-energy ratio (W/Wh)	9.4	12.5	15.6	18.8	21.9
0 to 60 mph time (s)	8.6	7.8	7.3	6.8	6.4

5.2 Influence on Control

Power directly affects regenerative braking, since a more powerful electric system can recuperate more energy from strong decelerations. This is all the more true as the cycle is aggressive, as shown in Figure 11. With 60% of original power, the vehicle captures 60% of the available energy, while this rate rises to 72% with 140% of original power. On the other hand, power scaling ratio has no influence on the regenerative braking energy recuperation on the UDDS and HWFET cycles.

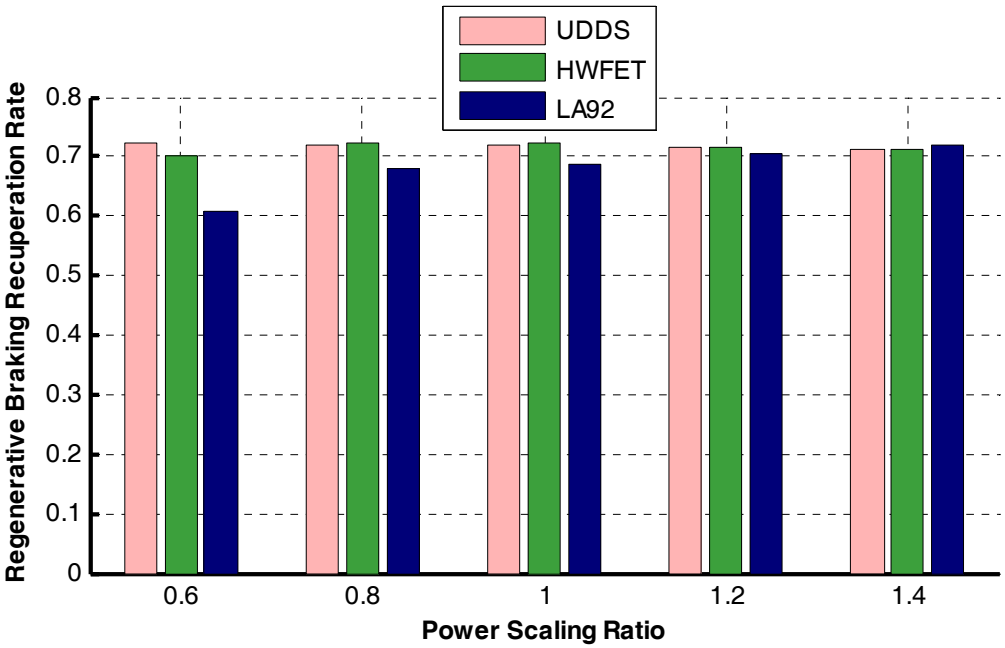

Figure 11: Regenerative braking recuperation rate – distance driven: 20 mi

Among the control parameters previously mentioned, the power demand at the wheels above which the probability of the engine being on is higher than 0.95 is the only parameter significantly affected by the power-scaling ratio. As can be observed in Figure 12, this threshold is lower for less-powerful vehicles. A lower-power electric system has less ability to propel the vehicle on its own, which results in longer engine running time.

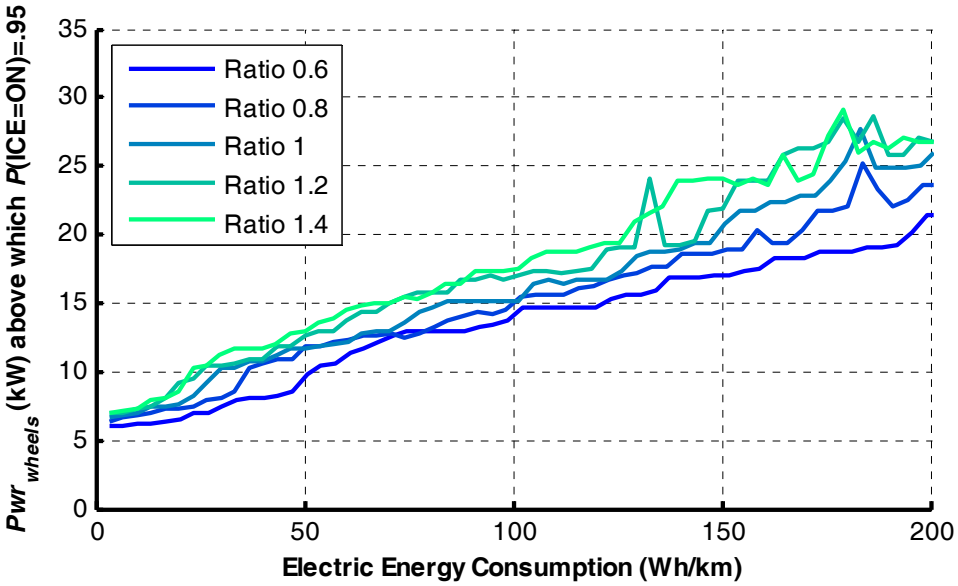

Figure 12: Power demand at the wheels above which ICE is on 95% of time – various ratios, UDDS: 20 mi

5.3 Influence on Fuel Economy and GHG

Figure 13 shows the minimal fuel consumption on several cycles, for the same driven distance of 10 mi, as well as the electric energy consumption at which this minimum is reached. As the power of the electric system decreases, so does the ability of the vehicle to run in EV mode, which results in an increased use of the engine and increased fuel consumption. That increase is all the more significant because the cycle is aggressive, as a result of the reduced rate at which regenerative braking energy is recuperated. Upsizing the electric components (power scaling ratios of 1.2 and 1.4) does not significantly change fuel consumption. On the other hand, downsized (power scaling ratios of 0.6 and 0.8) electric components have a greater impact and increase fuel consumption.

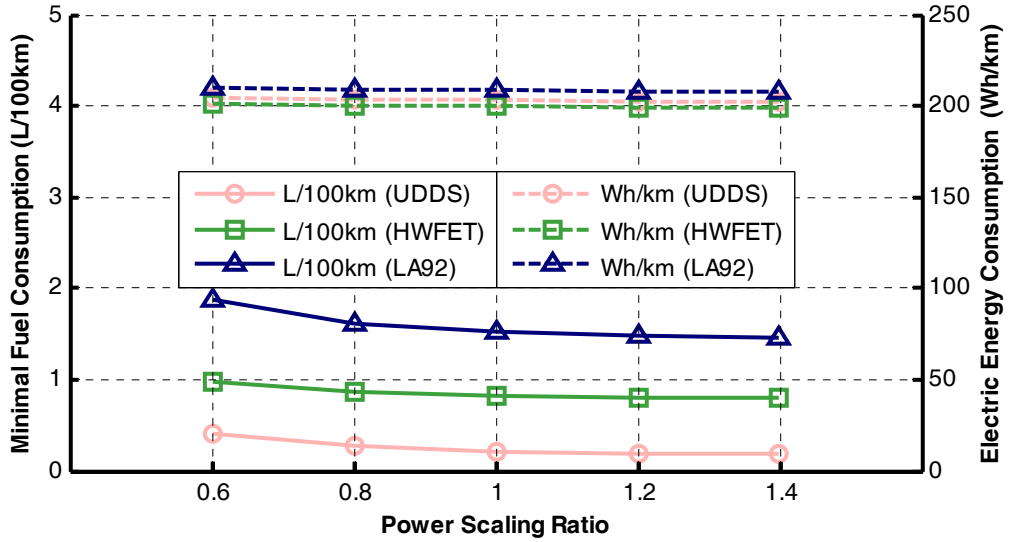

Figure 13: Minimal fuel consumption and associated electric consumption – distance driven: 10 mi

As shown in Figure 14, the power-scaling ratio may not affect GHG emissions. The high emissions of GHGs associated with electricity transportation and distribution in the 2010 American mix compensate for engine thermal losses.

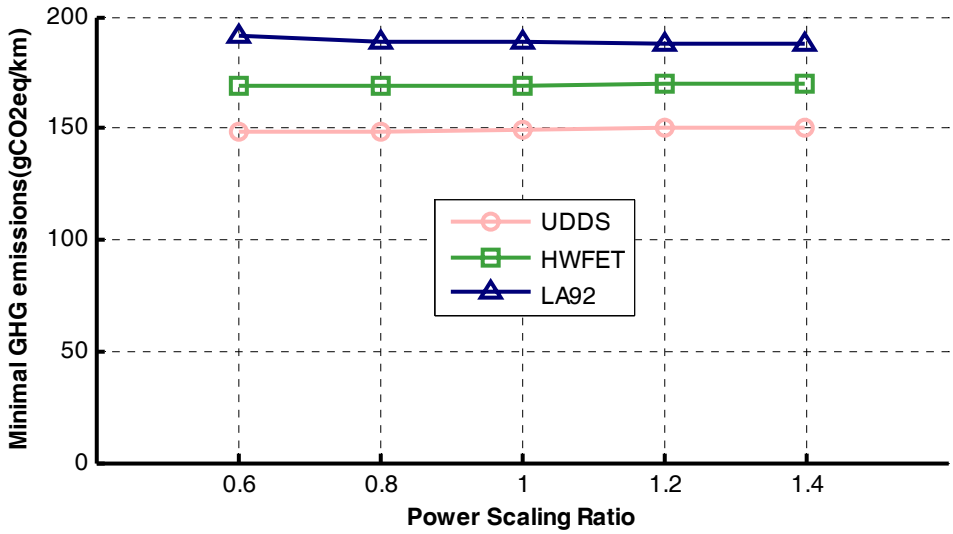

Figure 14: Minimal GHG emissions – distance driven: 10 mi

6 Conclusions

Global optimization allows a fair comparison of various vehicles because each of them is controlled optimally. The analysis of the control patterns showed common points. In particular, the wheel power demand threshold, which depends on the consumption of available electric energy, has been identified, and the engine operates at high efficiency when it is on. This gives a valuable indication for the design of actual rule-based controllers, because it is very common to link the decision to start the engine to the power demand at the wheels. The global optimization also showed that a charge-depleting mode is always preferred to an EV-mode followed by charge-sustaining mode.

Energy sizing, as expected, impacts the amount of fuel that can be displaced, because a vehicle with higher battery energy can rely longer on electricity before turning the engine on. On the other hand, power sizing — especially downsizing — impacts fuel displacement because lower electric power limits the regenerative braking energy, as well as the vehicle's ability to run in EV mode. Global optimization also allows assessment of the impact of component sizing on GHG emissions in a given electricity-generation scenario.

Future work will focus on extending the global optimization study, such as adding additional trips or including charge-sustaining optimal control, to generate a rule-based control that would maximize the fuel displacement under various driving conditions.

7 Acknowledgments

This work was supported by DOE's FreedomCAR and Vehicle Technology Office under the direction of Lee Slezak. The submitted manuscript has been created by UChicago Argonne, LLC, Operator of Argonne National Laboratory ("Argonne"). Argonne, a U.S. Department of Energy Office of Science laboratory, is operated under Contract No. DE-AC02-06CH11357. The U.S. Government retains for itself, and others acting on its behalf, a paid-up nonexclusive, irrevocable worldwide license in said article

We would like to thank Ye Wu for his inputs regarding the greenhouse gases emissions.

References

[1] Graham, B., "Plug-in Hybrid Electric Vehicle, A Market Transformation Challenge: the DaimlerChrysler/EPRI Sprinter Van PHEV Program," EVS21, April 2005.
[2] Shidore, N.; Bohn, T.; Duoba, M.; Lohse-Busch, H.; and Pasquier, M., "Innovative Approach to Vary Degree of Hybridization for Advanced Powertrain Testing using a Single Motor," EVS22, October 2006.
[3] Pagerit, S.; Rousseau, A.; and Sharer, P., "Global Optimization to Real Time Control of HEV Power Flow: Example of a Fuel Cell Hybrid Vehicle," EVS 21, April 2005.
[4] Karbowski, D.; Rousseau, A.; Pagerit, S.; and Sharer, P, "Plug-in Vehicle Control Strategy: From Global Optimization to Real Time Application," 22nd International Electric Vehicle Symposium (EVS22), Yokohama, October 2006.
[5] Argonne National Laboratory, PSAT (Powertrain Systems Analysis Toolkit), http://www.transportation.anl.gov/.
[6] Liot, C.; Fadel, M.; Grandpierre, M.; and Sans, M., "Global Energy Management for Vehicle In Gerico Project," EVS 21, April 2005.
[7] Deguchi, Y.; Kuroda, K.; Shouji, M.; and Kawabe, T., "HEV Charge/Discharge Control System Based on Navigation Information," SAE 2004-21-0028.
[8] Argonne National Laboratory, GREET 1.8a, http://www.transportation.anl.gov/software/GREET/.

Authors

Dominik Karbowski, Research Engineer, Argonne National Laboratory, 9700 South Cass Avenue, Argonne, IL 60439-4815, USA, dkarbowski@anl.gov , dominik.karbowski@mines-paris.org
Tel. 1-630-252-5362 / Fax: 1-630-252-3443

Dominik Karbowski works on vehicle systems modeling, simulation, and control at Argonne National Laboratory. He received a Master's degree in Science and Executive Engineering with an option in Energy Systems from the Ecole des Mines de Paris / ParisTech, France, in 2006.

Chris Haliburton, 402 Erb St West, Waterloo, Ontario Canada N2L 1W6
chris.haliburton@gmail.com

Chris Haliburton worked as a Research Assistant on vehicle systems modeling, simulation and control at Argonne National Laboratory. He is a candidate for a Bachelor's degree of Applied Science in Mechanical Engineering with an Option in Mechatronics from the University of Waterloo, Ontario Canada. Graduation date May 2008.

Aymeric Rousseau, Research Engineer, Argonne National Laboratory, 9700 South Cass Avenue, Argonne, IL 60439-4815, USA, arousseau@anl.gov
Tel. 1-630-252-7261 / Fax: 1-630-252-3443

Aymeric Rousseau is head of the Advanced Powertrain Vehicles Modeling Department at Argonne National Laboratory. He received his engineering diploma at the Industrial System Engineering School in La Rochelle, France, in 1997.